Chemical characteristics of inclusions formed at various stages during the ladle treatment of steel

K. Beskow, J. Jia, C. H. P. Lupis, and Du Sichen

Industrial data were analysed to shed some light on the formation and growth of non-metallic inclusions during the ladle treatment of a particular grade of tool steel, Orvar Supreme (Fe–0·39C–1·0Si–0·4Mn–5·2Cr–1·0Mo–0·9V). Seven types of inclusions were detected in samples taken along the processing evolution of the steel. The types of inclusions present were found to vary with the various stages of that evolution. While additions of aluminium to the steel bath were found to affect the composition of the inclusions, only a small number of pure alumina inclusions, agglomerated as clusters, were observed during the initial stages of deoxidation. Ladle glaze was found to be the major source of the inclusions. Most of those left in the steel before tapping were found to be of very small size and to contain high concentrations of Al_2O_3 and CaO and relatively minor ones of MgO and FeO. I&S/1671

Ms Beskow and Professor Du Sichen (du@metallurgi.kth.se) are in the Department of Materials Science and Engineering, Division of Metallurgy, Royal Institute of Technology, SE–100 44 Stockholm, Sweden and Mr Jia and Professor Lupis are in the Department of Materials Science and Engineering, Massachusetts Institute of Technology, Cambridge, MA, USA. Manuscript received 1 November 2001; accepted 12 March 2002.

INTRODUCTION

In the production of clean steels, the presence of non-metallic inclusions has become a major concern. Specifications of contents and sizes of inclusions in commercial steels vary with the product, e.g. from <5 μm diameter in ultraclean steels to <100 μm diameter in sheet steels.[1] A common goal, however, is to minimise the amount and size of the inclusions and to control their distribution in the final product.

Numerous investigations have been carried out in the past few decades to meet this goal. They can be classified into three groups: laboratory studies,[2–11] industrial investigations,[11–14] and mathematical modelling.[11,15–20] In view of the impact of the deoxidation process on the presence and nature of inclusions in the final product, most of these investigations[2–6,8–15,17,20] have naturally focused on that deoxidation operation.

Laboratory studies have mostly examined the behaviour of inclusions (in laboratory scale furnaces), particularly their mechanisms of formation and separation. Industrial investigations, on the other hand, have been mainly interested in obtaining their compositions, amounts, and size distributions, through statistical analyses and morphological characterisation. In both laboratory and industrial investigations, much effort has been expended on studying inclusions' collisions and agglomerations.

These collisions and agglomerations have also been subjected to mathematical modelling. Nevertheless, the development of process models and their optimisation with regard to inclusion engineering necessitate a deeper understanding of the behaviours of inclusions during the entire course of the process. Indeed, the results of laboratory studies cannot be incorporated into a process model unless the mechanisms of formation, growth, and separation of inclusions in a steelmaking process are well understood. Moreover, any meaningful modelling approach should also consider the operation of these mechanisms under realistic industrial conditions.

The present work is a preliminary study within a long term project to design a comprehensive process model of ladle treatment. It aims to understand the behaviours of inclusions along the history of the ladle process at Uddeholm Tooling AB in Hagfors, Sweden. Industrial data are analysed from a thermodynamic point of view. To discuss the results, the inclusions are classified into several types with respect to size, chemistry, and morphology.

PLANT TRIAL EXPERIMENTS

Process description

Uddeholm Tooling AB is a steel minimill operating with the use of scrap metal. Figure 1 shows a flow chart of the process before ingot casting. Between 35 and 65 t of scrap are melted in an electric arc furnace (EAF) and treated, if necessary, for phosphorus and carbon. The molten steel, having a temperature of $\sim$1670°C (1943 K), is tapped and transferred to the ladle furnace (LF) station, where it is deslagged. After deslagging, aluminium wire is introduced for deoxidation. In some cases, because of occasional breakdown of the wire unit, aluminium bars replace the wire. After deoxidation, various alloys are added, which depend on the specification of the steel grade. At the same time, alumet (20%CaO, 10%MgO, and 63%Al_2O_3), lime (68%Ca, 3·6%Mg, and 28·4%O), and dolomet (43%Ca, 24%Mg, and 33%O) are added to form a new top slag.

The ladle is heated to a temperature between 1580 and 1650°C (1853–1923 K), depending on the steel grade, and stirred by induction to ensure homogeneity. Once the alloys have dissolved and the appropriate steel composition has been attained, the steel temperature is adjusted to 1635°C (1908 K). The ladle is then transferred to a degassing station, where it is placed in a vacuum chamber and stirred by argon gas to eliminate nitrogen and hydrogen from the melt. Subsequently, the ladle is again stirred by induction to promote the growth and separation of inclusions from the steel into the slag. It is finally transferred to the casting station. Before casting, the steel has a temperature of $\sim$1570°C (1843 K).

Sampling technique

A particular steel grade, ORVAR SUPREME (Fe–0·39C–1·0Si–0·4Mn–5·2Cr–1·4Mo–0·9V), was chosen for the present work. Twelve to fourteen steel samples were taken for each heat, from the arrival of the ladle at the ladle station to the transfer of the ladle at the casting station. A rapid

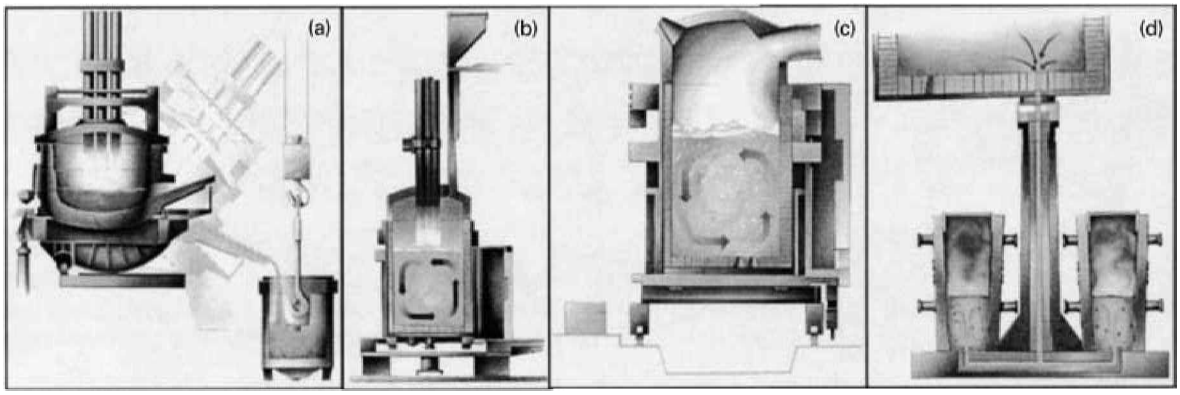

a electric arc furnace; *b* ladle furnace; *c* vacuum degassing; *d* uphill casting

1 Flow chart of steelmaking process at Uddeholm Tooling AB, Hagfors

solidification (RS) method was used to obtain the samples. An argon flow out of the sampler ensured that no slag would enter the sample holder. Once the sampler was in place in the melt, a vacuum drew the steel into the holder. Each steel sample was in the shape of a lollipop, as shown in Fig. 2.

The base of a sample was first polished and then three cuts were made near the head, creating three small lengths $\sim$0·5 cm in length and a long rod of varying length. The small pieces were used for carbon, sulphur, and oxygen analyses. The head was ground using 40 mm and 180 mm paper until the oxide layer was eliminated. This part was used for both composition analysis and microscopic examination. For each heat, slag samples were also taken at different stages of the process.

Sample analyses

Chemical compositions of steel samples

Carbon and sulphur contents were determined using a CS–444 LS carbon/sulphur determinator supplied by Leco Corp., Michigan, USA. A sample weighing between 0·5 and 1 g was used with a tungsten catalyst. Oxygen concentrations determined using equipment from Leco Corp. were affected by high uncertainties. This may have been caused by contamination during sampling. Therefore, in the analysis of experimental results, the oxygen concentrations of the steel samples have been disregarded.

While the concentrations of Mn, S, Cr, Ni, and Mo in the steel were determined by an ARL 8680 S SIM/SEQ X-ray fluorescence (XRF) spectrometer, the concentrations of Al, Ti, Ca, Mg, and B were determined by using an optical emissions spectrometer (OES), OBLF QS 750. For the latter concentrations, several data were taken and averaged.

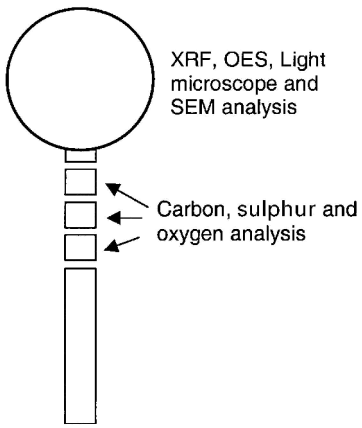

2 Steel sample in shape of lollipop: XRF X-ray fluorescence, OES optical emissions spectrometry

Chemical compositions of slag samples

Slag samples were ground into powder and cast into glass discs $\sim$3 cm in diameter. They were analysed using an XRF system (Phillips Perl X-2). The major oxide components were found to be CaO, Al_2O_3, SiO_2, MgO, and MnO. Sulphur was also detected.

Microscopic analyses of inclusions

Steel samples were examined under an optical microscope, and the inclusions found in these samples were further scrutinised under a scanning electron microscope (SEM). A Hitachi microscope model S-3500N, to which an energy dispersive X-ray (EDX) analyser (ISIS series 300, Oxford) had been added, was used. There were large uncertainties in the analyses of oxygen content using this technique, and, consequently, only the contents of metallic elements were retained to evaluate compositions of the inclusions. The results of these oxygen determinations, however, were still useful on a qualitative basis.

Measurements of oxygen activity

As mentioned above, analyses of oxygen concentration in the steel samples were subject to considerable uncertainties owing to contamination during sampling. Nevertheless, because of its importance, the oxygen activity in the metal bath was measured at various stages of the process using a Celox oxygen sensor (with a $Cr–Cr_2O_3$ reference electrode) supplied by Heraeus Electro-Nite.

RESULTS

Three heats of the steel grade, ORVAR SUPREME, were studied. Steel samples were taken at different stages of the process:

(i) on arrival of the ladle at the ladle furnace (LF) station
(ii) after deslagging
(iii) during aluminium addition
(iv) after aluminium addition

Table 1 Oxygen activity in steel melt during various process steps

Stage*	Oxygen activity with respect to 1 wt-% dissolved oxygen as reference state
1 Before deoxidation and alloying in EAF	0·02–0·05
2 Before deslagging in LF	0·001
3 After Al addition	0·0001–0·0002
4 Before vaccum	0·0001–0·0004
5 After vaccum	0·0001–0·0002

*EAF is electric arc furnace, LF is ladle furnace.

Table 2 Compositions* of steel samples corresponding to various process steps, wt-%

Stage	C	Si	Mn	P	S	Cr	Mo	Ni	Al	B	Co	Cu	N	Ti	V	Ca	Ce	Sn
1	...	...	...	...	...	...	...	...	...	...	...	...	...	...	...	...	...	...
2	0·21	1·03	0·12	0·005	0·008	2·81	1·28	0·14	0·001	0·0001	0·04	0·13	0·011	0·002	0·006	0·0003	0·003	0·006
3	0·22	1·04	0·12	0·006	0·008	2·82	1·29	0·14	0·034	0·0001	0·04	0·13	0·01	0·002	0·007	0·0003	0·003	0·007
4	0·33	1·07	0·39	0·008	0·006	5·1	1·46	0·14	0·065	0·0001	0·04	0·13	0·015	0·0023	0·93	0·0002	0·003	0·006
5	0·4	1·14	0·39	0·009	0·0014	5·12	1·46	0·14	0·02	0·0001	0·04	0·13	0·009	0·0025	0·94	0·0002	0·003	0·005

*Mg concentration is ~0·0002 wt-%.

(v) after alloying
(vi) before vacuum degassing
(vii) after degassing.

Although aluminium bars were used in the first two heats and wire injection was used in the third, experimental results for the three heats were similar.

Oxygen activities were measured at various stages of the ladle treatments and in the EAF before deoxidation and alloying. The results are listed in Table 1. The compositions of the steel samples taken at the various stages are given in Table 2.

To obtain an insight into the effect of slag composition on the inclusions, slag samples were taken before deslagging, and also before and after the vacuum degassing process. The corresponding analyses are given in Table 3.

The inclusions found in the steel samples have been classified into seven categories, A–G. Figure 3 presents typical micrographs of these categories. Their compositions and size ranges are listed in Table 4. Note that the compositions given are affected by experimental uncertainties. In the EDX analyses, uncertainties resulted from the small sizes of the inclusions. Indeed, when the size of an inclusion is about the same as the diameter of the EDX beam, the results can only be treated as semiquantitative. This is particularly true in the case of FeO contents.

Description of inclusions

Inclusions of type A have a perfectly spherical shape as shown in Fig. 3*a*. No substantial concentration gradient was detected in each sphere, although the compositions differ somewhat from one inclusion to another. The spherical shape of the inclusions and their homogeneity suggest that type A inclusions are liquid.

Table 3 Analysed slag composition before deslagging in ladle furnace (LF), before and after vacuum treatment, wt-%

Heat	Stage	CaO	Al_2O_3	SiO_2	MgO	FeO
1	Before deslagging in LF	40·3	15·9	19·2	17·6	2·4
	Before vacuum	46·3	27·4	10·6	10·9	1·2
	After vacuum	47	32·1	8·7	9·7	0·2
2	Before deslagging in LF	43	7	29·9	16·8	0·7
	Before vacuum	54·9	23·9	9·4	8·9	0·2
	After vacuum	52·1	28·3	7·8	8·3	0·3

This conclusion is supported by consideration of the compositions of these inclusions with respect to the phase diagram of the Al_2O_3–CaO–MgO–SiO_2 system[21] shown in Fig. 4, assuming that FeO plays an equivalent role to CaO. Although the FeO content in these inclusions is fairly high, the above assumption is necessitated by the apparent absence of phase diagram information for the Al_2O_3–CaO–FeO–MgO–SiO_2 system. Note also that additions of moderate amounts of FeO are generally expected to decrease the liquidus temperature of the slag.

Inclusions of type B contain only Al_2O_3 and MgO. Compositions of these inclusions were found to vary within the stoichiometric range of the spinel phase Al_2O_3.MgO (*see* phase diagram in Fig. 5.)

Inclusions of type C, shown in Fig. 3*c*, consist of two phases and appear to be a combination of types A and B. The Al_2O_3.MgO spinel is surrounded by a liquid phase that has a composition range similar to that of type A.

Inclusions of type D contain Al, Mg, and Fe oxides, and EDX analyses showed them to exhibit considerable concentration gradients and higher FeO contents at the surface. The chemical compositions of these inclusions indicate that they correspond to the phase Al_2O_3.(Fe,Mg)O, a ternary solid solution in the Al_2O_3–MgO–FeO system, probably along the Al_2O_3.FeO–Al_2O_3.MgO composition line.

Both types B and D have a spinel structure. These two types of inclusions belong, possibly, to the same structure along the Al_2O_3.FeO–Al_2O_3.MgO composition line. The B type inclusions differ from the D type inclusions by the absence of FeO in the solid solutions.

Only a few inclusions of type E were found in the samples taken in the vicinity of aluminium additions during the deoxidation period. These inclusions were found to consist of pure alumina and to be in the form of clusters (i.e. a number of small particles attached to each other, Fig. 3*e*).

Inclusions of type F appear to have two layers: a spinel phase in the centre, surrounded by a layer containing Al_2O_3, CaO, MgO, and small amounts of FeO. The Al_2O_3.MgO spinel phase in the centre of the inclusions is the same as that in the B inclusions. In the outer layer of these type F inclusions, the Al_2O_3 content is very high and approximately constant (mole fraction 0·5), while the concentrations of CaO, FeO, and MgO vary (as indicated in Table 4). The almost constant alumina content implies

Table 4 Compositions (mole fraction and wt-%) and size ranges for inclusion types A–G

		Al_2O_3		MgO		CaO		SiO_2		FeO	
Inclusion type	Size, μm	mole fraction	wt-%	mole fraction	wt-%	mole fraction	wt-%	mole fraction	wt-%	mole fraction	wt-%
A	2–7	0·22–0·3	30–43	0·1–0·2	6–12	0·06–0·16	5–13	0·13–0·16	11–14	0·25–0·45	29–45
B	4–10	0·57–0·65	77–82	0·35–0·43	18–23	...	...	...	...	...	...
C	8–20	0·5–0·6	72–80	0·4–0·5	20–28	...	...	...	...	...	...
	(few <8)	0·25–0·35	38–50	0·1–0·3	5–16	0·1–0·3	7–22	0·1–0·25	9–20	0·1–0·3	10–30
D	2–6	0·4–0·5	55–70	0·3–0·4	15–20	...	...	...	...	0·2–0·3	20–30
E	10–40	1	100	...	...	...	...	...	...	...	...
F	2–25	0·6–0·64	79–83	0·36–0·4	17–21	...	...	...	...	...	...
		0·5–0·57	65–77	0·1–0·25	5–13	0·15–0·4	10–27			0–0·1	0–9
G	2–6 (few 15–20)	0·28–0·35	42–50	0·1–0·15	6–9	0·5–0·6	39–50	0–0·05	0–4	...	...

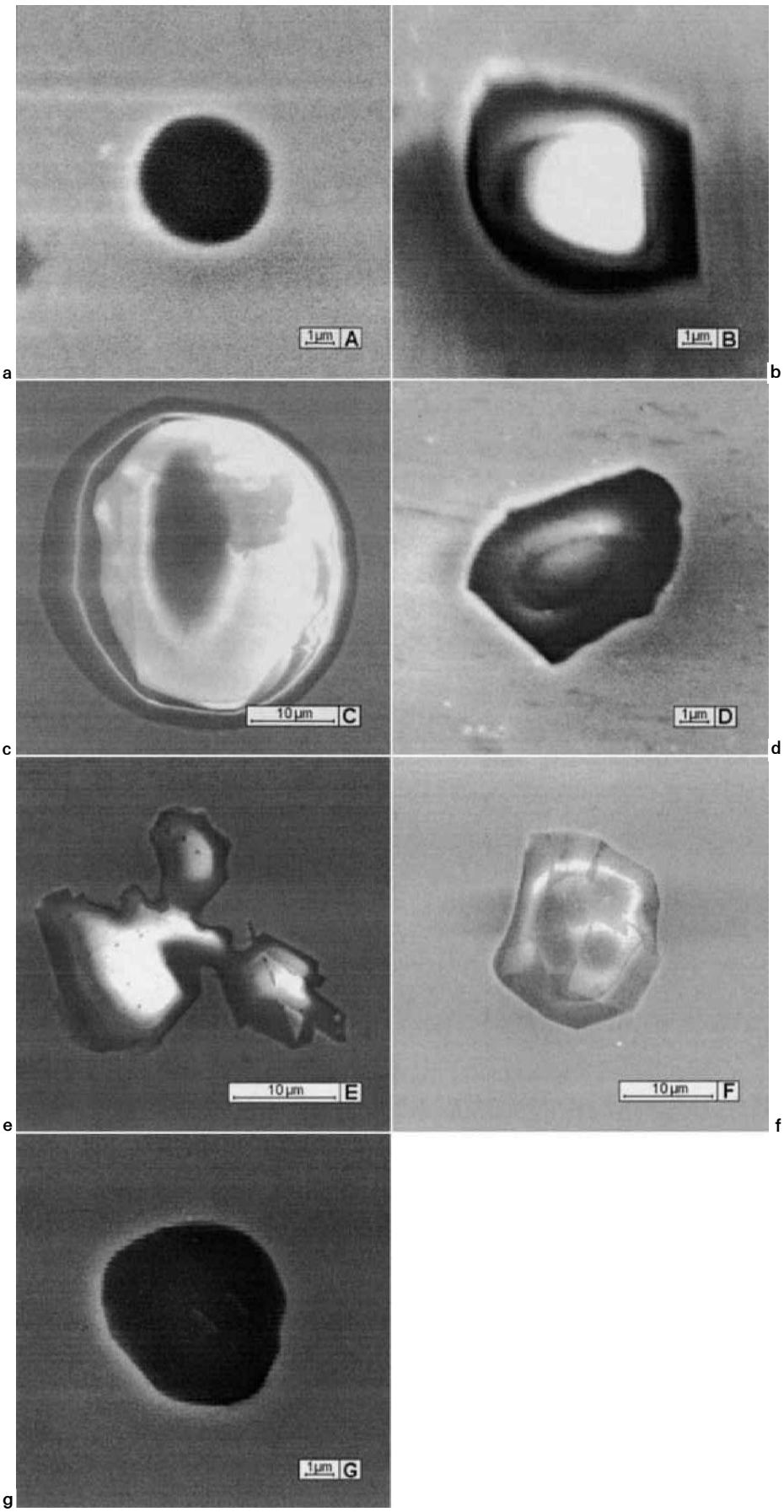

a A; *b* B; *c* C; *d* D; *e* E; *f* F; *g* G

3 Micrographs of given inclusion types

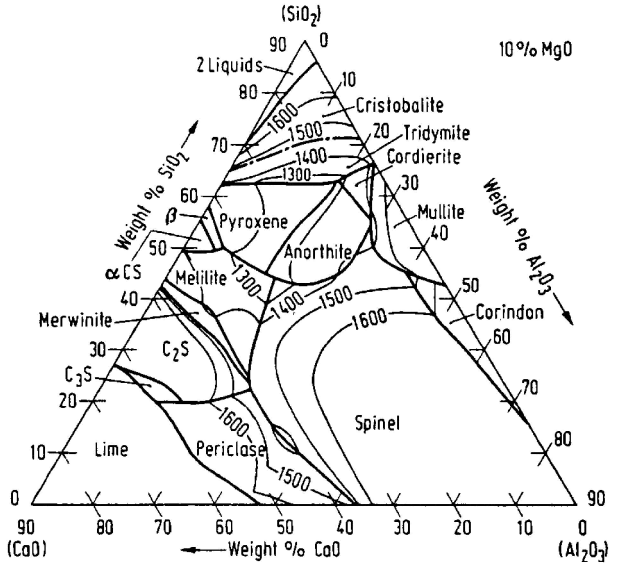

4 Phase diagram of Al_2O_3–CaO–MgO–SiO_2 system: after Ref. 21

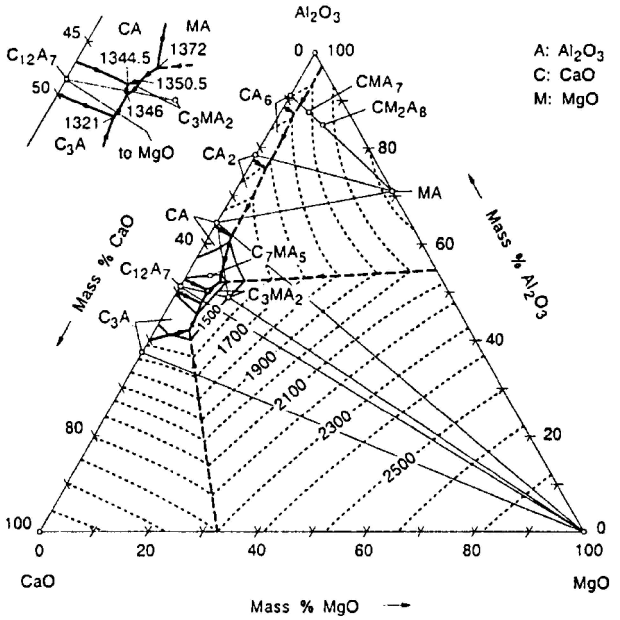

6 Phase diagram of Al_2O_3–CaO–MgO system: after Ref. 21

that, probably, this layer is also a spinel. Thus, it appears that inclusions of type F consist of a spinel phase with Al_2O_3.MgO in the centre and increasing FeO and CaO concentrations towards the surface.

Most of the inclusions of type G are very small (2–6 μm), although some bigger particles were observed. As in the case of the outer layer of type F, they contain Al_2O_3, CaO, and MgO, but small amounts of FeO. Because most of these inclusions are very small, the FeO concentrations provided by EDX analysis are unreliable and thus not reported in Table 4. In contrast with the outer layer of type F inclusions, the content of CaO is very high (~50 mol-%), which distinguishes these inclusions from those of type F.

The composition range of type G inclusions indicates that they are unlikely to correspond to a spinel structure. The phases in these inclusions are difficult to identify because information on the phase diagram of the Al_2O_3–CaO–FeO–MgO system is lacking. Even information on the phase relationships in the subternaries, such as Al_2O_3–CaO–MgO and Al_2O_3–CaO–FeO, is incomplete.

The phase diagram of the Al_2O_3–CaO–MgO system,[21] reproduced in Fig. 6, indicates the existence of a ternary compound, $2Al_2O_3.3CaO.MgO$, first reported by Majumdar[22] and later confirmed by Glasser and Marr.[23] This compound, which has molar ratios of Al_2O_3/CaO/MgO similar to those observed in type G inclusions, may accept some FeO in solution. It is possible, however, that another quaternary compound, with molar ratios close to those of the $2Al_2O_3.3CaO.MgO$ compound, exists in the Al_2O_3–CaO–FeO–MgO system.

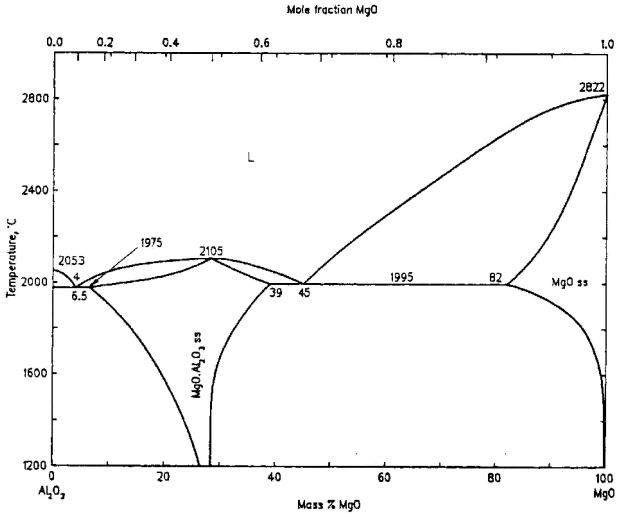

5 Phase diagram of Al_2O_3–MgO system: after Ref. 21

DISCUSSION

Figure 7 illustrates the types of inclusions found at various stages of the ladle treatment.

Before aluminium addition

In samples taken before aluminium addition, four types of inclusions were observed, those of types A, B, C, and D. As mentioned above, type A inclusions must have been liquid when the steel samples were taken. A comparison of their chemical composition with that of the EAF slag in Table 3 shows that they differ considerably from each other. In particular, the concentration of CaO in the inclusions is much lower than that in the slag, while the Fe concentration is much higher. This would rule out the possibility that the liquid inclusions were introduced by slag entrainment into the liquid metal either during the tapping of the EAF or during the sampling. Hence, either type A inclusions would already have been in the steel bath in the EAF, or they would have been flushed into the liquid steel from the ladle glaze.

A ladle glaze is a thin coating of slag formed when the top slag is in contact with the ladle lining during the draining of the ladle. A number of studies[24–28] have been carried out to investigate the effect of ladle glazes on the formation of inclusions. Indeed, a recent investigation by Riaz *et al.*[28] has shown strong experimental evidence that ladle glazes are a major source of inclusions in liquid steel. The authors used an Al_2O_3–CaO–MgO–SiO_2 slag and a carbon bearing MgO lining and reported that, after the slag–refractory reaction, two distinct layers were observed above the decarburised refractory layer. The first layer consisted of an Al_2O_3–CaO–MgO–SiO_2 slag with an increasing MgO content as the slag descended. The second layer, immediately below the first and in contact with the lining, consisted of two phases, a spinel and a slag.

It is reasonable to believe that in the present ladle treatment, ladle glaze was also the major source of inclusions, especially type A. The operation at Uddeholm used an

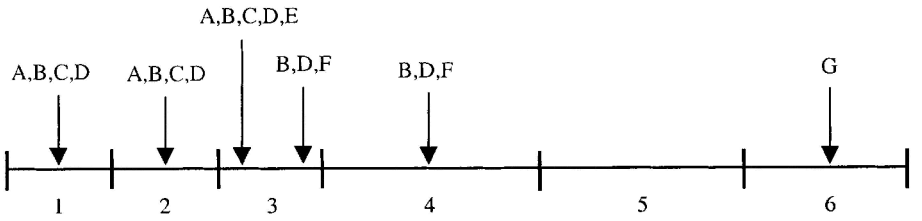

1: before deslagging; 2: after deslagging; 3: deoxidation; 4: alloying period; 5: degassing; 6: after degassing

7 Types of inclusions found at given stages of ladle treatment: A–G denote inclusion types

Al_2O_3–CaO–MgO–SiO_2 slag and carbon bearing MgO linings, conditions very similar to those of Riaz *et al.*[28] At high temperatures, the slag would be expected to react with the refractory lining of the ladle. Moreover, some liquid iron would adhere to the wall instead of being drained by the descending steel, and would react with the descending slag. This would lead to changes in the composition of that liquid slag, subsequently frozen upon cooling of the ladle.

With another cast of steel poured into the glazed ladle, the adhered glaze layer would be removed and the frozen slag would be remelted. Part of the remelted slag, in the shape of small drops, would be entrained in the liquid metal forming type A inclusions. The composition of the frozen slag in the glaze layer would be locally homogeneous, but would change with its position in the ladle, which is in accordance with the observation that in each type A inclusion the composition was homogeneous but varied somewhat from one inclusion to another.

Most, if not all, inclusions of types B and C could also originate from the ladle glaze. As reported by Riaz *et al.*,[28] the second layer of the glaze is a two phase mixture consisting of spinel and liquid slag. Upon removal of the glaze layer, the small spinel particles would be entrained along with the slag into the liquid metal. While the bigger spinel particles would float to the surface, the smaller ones would remain in the steel as inclusions. Depending upon the way in which they were detached from the refractory wall (and their position there), the spinel inclusions would be associated with some slag or be free of it. In the latter case they would be type B inclusions and in the former case type C. The observed configuration of type C inclusions, a nearly spherical volume of liquid slag with a spinel core, is undoubtedly dictated by a minimisation of the interfacial free energy.

To identify the source of type D inclusions, it would be helpful to estimate the oxygen potential required for the formation of these inclusions. Unfortunately, there is no phase diagram information for the Al_2O_3–FeO–MgO system. As mentioned above, EDX analyses showed that this type of inclusion appeared to be a ternary solution. It may be noted that the Al_2O_3–FeO–MnO system exhibits a solid solution along the $Al_2O_3.FeO$–$Al_2O_3.MnO$ composition line. In view of the similarity of MnO and MgO, it is reasonable to expect that inclusions of type D could be a solution along the $Al_2O_3.FeO$–$Al_2O_3.MgO$ composition line. It is very difficult to evaluate accurately the oxygen potential in equilibrium with that ternary solution. However, a calculation based on the formation of $Al_2O_3.FeO$ would help in understanding the formation of type D inclusions. Oxygen activities in liquid iron can be calculated for different activities of alumina on the basis of the following reaction

$$Al_2O_3 + Fe(l) + \underline{O}\ (\text{wt-}\%) = Al_2O_3.FeO;$$

$$\Delta G^\circ = -48\,650\ (\text{J}) \quad \ldots\ldots\ldots\ldots\ldots\ldots\ (1)$$

where ΔG° is the Gibbs free energy of formation for the reaction. The underline denotes a Henrian standard state for the oxygen (dissolved in liquid iron) on a weight per cent basis. The equilibrium constant for equation (1) can be described by:

$$K = \frac{a_{Al2O3.FeO}}{a_{Al2O3}\, a_{Fe}\, a_O} \quad \ldots\ldots\ldots\ldots\ldots\ (2)$$

On the basis of equation (2), activities a_O of oxygen were calculated for different activities a_{Al2O3} of alumina. In the calculation, the activities of $Al_2O_3.FeO$ and iron were assumed to be 1. In Fig. 8, the equilibrium oxygen activity is plotted as a function of the activity of alumina at 1873 K. The thermodynamic data used for these calculations were taken from Refs. 29–31. It is seen from Table 1 that the oxygen concentration in the EAF can be as high as 500 ppm before deoxidation and alloying. The formation of $Al_2O_3.FeO$ would be possible in the EAF. This compound would even be thermodynamically stable after the decarburisation period. In addition, if a solid solution $Al_2O_3.(Fe,Mg)O$ is formed, the activity of $Al_2O_3.FeO$ would be lower, and a decrease in the $Al_2O_3.FeO$ activity would further favour reaction (1) above. The contact of the refractory (MgO + C) with the slag in the EAF would provide sites for the formation of the $Al_2O_3.(Fe,Mg)O$ phase.

Deoxidation period

Not surprisingly, in the initial stage of the deoxidation period, inclusions of types A, B, C, and D were still found in the liquid steel. In addition, however, inclusions of type E were also observed. These, as illustrated in Fig. 3*e*, clearly show agglomeration of alumina particles during the addition of aluminium. It is worthwhile mentioning that the steel sample containing the inclusion shown in Fig. 3*e* was taken near the spot where aluminium bars were added, and within 1 min of that addition. The existence of such inclusions provides evidence of homogeneous nucleation of Al_2O_3 according to the reaction

$$2\underline{Al}\ (\text{wt-}\%) + 3\underline{O}\ (\text{wt-}\%) = Al_2O_3 \quad \ldots\ldots\ (3)$$

This observation is in accordance with earlier findings.[3,2] The presence of alumina clusters within 1 min of the aluminium

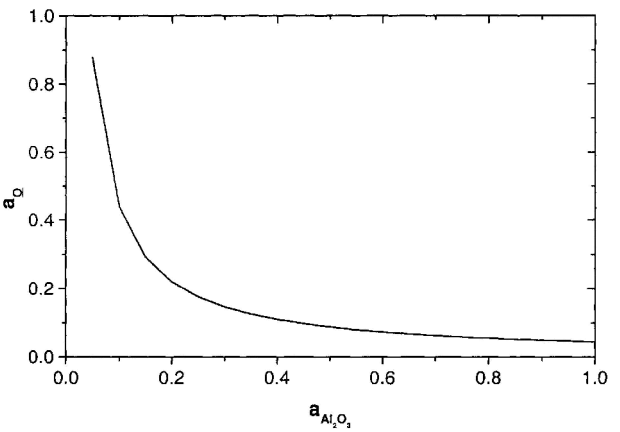

8 Equilibrium oxygen activity a_O as function of activity of alumina $a_{Al_2O_3}$ at 1873 K for reaction (1): spinel $Al_2O_3.FeO$ is stable in domain above curve

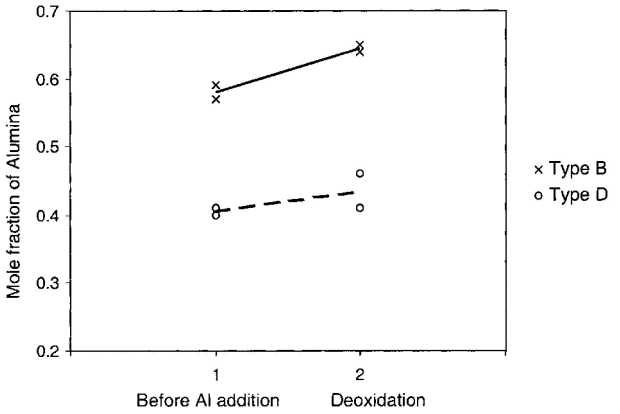

9 Variation of alumina content (mole fraction) in inclusions of type B and type D from start of ladle treatment to period of deoxidation

addition indicates that the process of agglomeration is fairly rapid. This can be explained by a high local aluminium concentration, leading in turn to a large local population of Al_2O_3 nuclei.[32] The observation that only a small number of type E inclusions were found, and only in steel samples taken in the vicinity of the aluminium additions, supports this rationalisation.

In later stages of the deoxidation period, only inclusions of types B, D, and F were observed in the steel samples. In inclusions of both types B and D, the alumina concentration appears to have increased as illustrated in Fig. 9. Note that in the phase diagrams of the Al_2O_3–MgO and Al_2O_3–FeO systems[21] shown in Figs. 5 and 10, respectively, both Al_2O_3.MgO and Al_2O_3.FeO phases exhibit a range of non-stoichiometry. Thus, when aluminium is added to the melt, both Al_2O_3.MgO and Al_2O_3.FeO particles could behave as favourable nucleation sites. The surfaces of the particles would then be enriched in Al_2O_3, which would diffuse into the bulk, resulting in an increase of the aluminium content of the inclusion.

The presence of type F inclusions can be explained by the dissolution of CaO and FeO into the Al_2O_3.MgO phase. Since Fe^{2+}, Mg^{2+}, and Ca^{2+} are similar basic cations, CaO and FeO would tend to dissolve into the Al_2O_3.MgO phase to form quaternary spinel solid solutions. Because there is no information of the phase diagram of the Al_2O_3–CaO–FeO–MgO system, thermodynamic calculations for this type of inclusions would be difficult. It is expected, however, that CaO and FeO would be formed on the surface of an inclusion's Al_2O_3.MgO spinel and that these two oxides would further diffuse into the inclusions because of potential gradients.

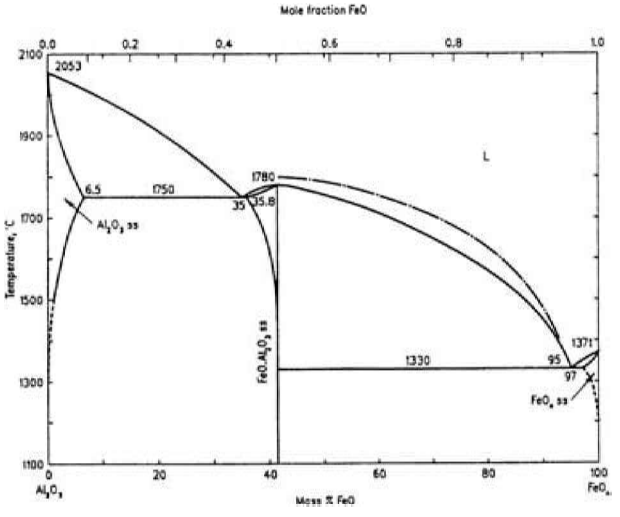

10 Phase diagram of Al_2O_3–FeO system: after Ref. 21

It is interesting to note that pure alumina inclusions were not found in steel samples associated with the later stages of deoxidation. The sharp decrease of oxygen concentration owing to the initial addition of aluminium would lead to a large decrease of the driving force for the formation of alumina nuclei. Hence, the probability for homogeneous nucleation of alumina would be very low in the later stages of deoxidation. Consequently, the dissolved oxygen and aluminium would prefer to react on the surfaces of inclusions of types B and D, thereby increasing their Al_2O_3 contents.

The observed disappearance of inclusions of type A and type C at this processing stage of the steel could be due to the collision and growth of the inclusions, which allow the easy flotation, and therefore separation, of the inclusions. Another possibility is that the dissolved aluminium would reduce FeO and SiO_2 in these liquid drops. The reduction would decrease the SiO_2 and FeO contents in the inclusions and lead to an increase of the liquidus temperature, resulting in solid inclusions. However, a comparison of the CaO content in the type D inclusions with that in type A would rule out the possibility that type D is the reduction product. In the case of type B and type F, both inclusions had extremely low SiO_2 content. If the liquid inclusions had been reduced, they would have yielded some solid inclusions with a certain concentration of SiO_2. A thermodynamic calculation was carried out to evaluate the lowest possible SiO_2 concentration on the basis of the reaction

$$2\underline{Al}\ (\text{wt-}\%) + 3/2SiO_2\ (\text{in slag}) = 3/2\underline{Si}\ (\text{wt-}\%) + Al_2O_3\ (\text{in slag}) \quad (4)$$

$$\Delta G^0_4 = -227\,875\ (\text{J}) \quad (5)$$

For this calculation, a slag model developed earlier in the present laboratory[33] was employed to evaluate the activities of oxides in the liquid, while the activities of silicon and aluminium in the liquid metal were calculated using a dilute solution model. The equilibrium constant K for equation (4) can be described as

$$K = \frac{a_{Al2O3}[f_{Si}\ (\text{wt-}\%\text{Si})]^{3/2}}{(a_{SiO2})^{3/2}[f_{Al}\ (\text{wt-}\%\text{Al})]^2} \quad (6)$$

where f_{Al} and f_{Si} are the activity coefficients of aluminium and silicon, respectively, and can be expressed by

$$\log_{10} f_i = \sum_{j=2}^{m} e_i^j\ (\text{wt-}\%j) \quad (7)$$

where e_i^j is the interaction parameter of j on i.[34,35] The contents of the elements in the steel used in the calculation can be found in Table 2. The corresponding interaction coefficients used are listed in Table 5. The Gibbs free energies of the oxides and dissolutions were obtained from Sigworth and Elliott and Stull and Prophet.[34,36] The calculation revealed that the lowest possible activity of SiO_2 was $\sim$0·0036, which would correspond to a SiO_2 content of a few per cent.[33] A comparison of this result with the extremely low content of SiO_2 in the inclusions of type B and type F would suggest that neither type B nor type F would be the product of reaction (4). Hence, it is concluded that the vanishing of inclusions of types A and C was not due to the reduction reactions. Collision and growth followed by flotation could be expected to be the main mechanism of disappearance of inclusions types A and C.

Alloying period

The types of inclusions found during this period were the same as observed in the later stages of deoxidation, namely type B, type D, and type F. Additions of alloys into the ladle did not affect the chemistry of the inclusions to any appreciable extent.

After degassing

After ladle treatment, most inclusions had been separated from the liquid steel. The only inclusions found after degassing were type G, most of which were very small. As mentioned above, inclusions of type G have substantially higher CaO content, compared with inclusions of type F. There are two possibilities for the presence of this type of inclusion. Alumet was one of the raw materials used to obtain the synthetic slag. This material contains high contents of alumina (63 wt-%) and CaO (20 wt-%) with 10 wt-% of MgO. If some fine particles of this material were entrained into the liquid steel before they reacted with the other raw materials, these tiny particles might be left in the steel as inclusions. However, a comparison of the composition of alumet with the composition of the inclusions of type G indicates that the CaO content in the inclusions is too high. This comparison would indicate that if alumet was one of the major sources of inclusions of type G, it would have had to undergo a process of chemical reaction during the degassing period, which is about 30 min.

It is more likely that the inclusions of types B, D, and even F reacted with the dissolved calcium to form inclusions of type G. The absence of inclusions of types B, D, and F before tapping would imply that the quaternary phase present in type G inclusions is thermodynamically more stable than the spinel phase under the degassing conditions. The long degassing time and the fine particle size would facilitate the reaction process. This argument can also hold for alumet particles.

A quantitative thermodynamic calculation is difficult owing to a lack of information on the phase present in inclusions of type G. Even thermodynamic data for the compound $2Al_2O_3.3CaO.MgO$ are unavailable. However, a comparison of the Gibbs free energies of formation for $Al_2O_3.MgO$ and $Al_2O_3.CaO$ would throw some light on the stability of the $Al_2O_3.MgO$ spinel. The Gibbs free energy of formation of $Al_2O_3.MgO$ from its oxide components[34,36,37] is $-28\,767$ J, which is less negative than the Gibbs free energy of formation of $Al_2O_3.CaO$ ($-54\,295$ J) from Al_2O_3 and CaO. Thermodynamic calculation on the basis of the composition of the steel sample taken before degassing shows that $Al_2O_3.CaO$ is more stable than $Al_2O_3.MgO$ in the melt when the following reaction is considered

$$\underline{Ca}\ (\text{wt-}\%) + Al_2O_3.MgO = \underline{Mg}\ (\text{wt-}\%) + Al_2O_3.CaO \quad \ldots\ldots\ldots (8)$$

$$\Delta G_8^0 = -157\,195\ (\text{J}) \quad \ldots\ldots\ldots (9)$$

Table 5 Interaction coefficients[34,35]

	Element *i*			
Element *j*	Al	Si	Ca	O
C	0·091	0·18	−0·34	−0·45
Si	0·0056	0·11	−0·1	−0·131
Mn		0·002		−0·021
P		0·11		0·07
S	0·03			−0·133
Cr		−0·0003		−0·04
Ni			−0·044	0·006
Mo				0·0035
Co				0·008
V				−0·3
Ti				−0·6
Cu				−0·013
Sn		0·017		−0·011
Al	0·045	0·058	−0·072	−3·9
Ce				−0·03
N		0·005		
Be				
Ca	−0·047	−0·087	−0·002	
O	−6·6	−0·23		−0·2

In the calculation, the dilute solution model of equation (7) is employed to evaluate the activity of calcium in the steel using the data listed in Tables 2 and 5. Assuming that the activities of $Al_2O_3.CaO$ and $Al_2O_3.MgO$ are both 1, the equilibrium activity of magnesium is calculated to be 0·047 (Henrian standard state, on weight per cent basis), which is more than 200 times the magnesium concentration in the liquid steel.

Furthermore, the vapour pressure of magnesium (20 atm) is one order of magnitude higher than the vapour pressure of calcium (1·9 atm) at 1873 K.[38] During vacuum degassing, volatilisation of magnesium from the liquid steel would favour the displacement of reaction (8) to the right, that is the replacement of $Al_2O_3.MgO$ by $Al_2O_3.CaO$.

Although the above thermodynamic analysis is based on $Al_2O_3.CaO$ but not the phase in the inclusions of type G, it still demonstrates that the spinel phase in inclusions of type B and even type D is not the most stable phase during vacuum treatment. To elucidate the presence of inclusions of type G, it would be necessary to identify the phase in the G type inclusions and to obtain thermodynamic data for it.

Note that the vanishing of inclusions types B, D, and F during vacuum degassing by flotation to the surface could be affected by many factors, such as the size of the inclusions, and the interfacial tensions between the inclusions and metal as well as between the inclusions and slag. The interfacial tension between inclusions and argon gas has been found to have an important influence on separation of the inclusions.[39–41] In the present ladle treatment, the argon bubbles might also have an important function in the separation of the inclusions. The influence of all these factors will be the next step of the present research programme.

The above discussion indicates that the addition of aluminium has a great impact on the inclusion chemistry. Deoxidation of the steel bath by aluminium results not only in alumina inclusions, but also in composition changes in inclusions of types B and D. While evidence of homogeneous nucleation of Al_2O_3 followed by the agglomeration of alumina particles is observed during the initial period of deoxidation, the number of agglomerated alumina inclusions is limited. The rapid vanishing of pure alumina inclusions suggests that the separation of pure alumina inclusions would not require special consideration, with reference to the tap time of the ladle treatment at Uddeholm Tooling. On the other hand, the separation of inclusions of type G plays a key role in keeping the steel clean when it leaves the ladle.

The major sources of inclusions of type G are expected to be the ladle glaze and, probably, inclusions from both the EAF and raw materials. The number of such inclusions in the steel before tapping would thus depend on several factors, namely the initial concentration of inclusions, the glaze history, the manner by which alumet is added, the degassing time, and the physical properties of the inclusions and the slag. Since the composition of the steel and the oxygen potential in the system have great impact on the growth and composition of the inclusions, they would also affect the final number and size distribution of inclusions in tool steels.

SUMMARY

Industrial trial studies were carried out at Uddeholm Tooling AB, Sweden, to investigate the formation and behaviour of inclusions during ladle treatment. The experimental results were analysed thermodynamically to gain an insight into the origins of the inclusions and their change along the stages of the ladle treatment. The addition of aluminium was found to have great impact on the inclusion chemistry. Deoxidation of the steel bath by aluminium resulted not only in alumina inclusions, but also in composition changes in spinel type inclusions. While evidence of

homogeneous nucleation of Al_2O_3 followed by agglomeration of alumina particles was observed during the initial period of deoxidation, the number of agglomerated alumina inclusions was limited. Indeed, pure alumina inclusions were found to vanish very rapidly. The present investigation indicates that ladle glaze plays an important role in introducing inclusions of spinel types. Only one type of inclusion, possibly a quaternary solid solution of Al_2O_3, CaO, FeO, and MgO, was observed before tapping.

ACKNOWLEDGEMENTS

The authors would like to thank especially Dr M. Nzotta and H. Issal for their help in the trial experiments. The authors are grateful to Professor S. Seetharaman for his illuminating suggestions and discussion during this work. The authors also acknowledge Professor P. Jönsson for his comments on the manuscript. Facilities provided by Uddeholm Tooling AB for this investigation are appreciated. Financial support for this work from both the Swedish Council for Technical Science (TFR) and Uddeholm Tooling AB is gratefully acknowledged.

REFERENCES

1. A. W. CRAMB: in 'Impurities in engineering materials', (ed. C. L. Braint), 49–90; 1999, New York, Marcel Dekker.
2. T. KAWAWA and M. OHKUBO: *Trans. Iron Steel Inst. Jpn,* 1968, **8**, 203–219.
3. K. MUKAI, H. SAKAO, and K. SANO: *Trans. Iron Steel Inst. Jpn*, 1969, **9**, 196–202.
4. K. MUKAI, H. SAKAO, and K. SANO: *Trans. Iron Steel Inst. Jpn*, 1969, **9**, 203–215.
5. G. K. SIGWORTH and J. F. ELLIOTT: *Metall. Trans.* 1973, **4**, 105–113.
6. H. FREDRIKSSON and Ö. HAMMAR: *Metall. Trans. B*, 1980, **11B**, 383–408.
7. K. HIGASHITANI, K. YAMAUCHI, Y. MATSUNO, and G. HOSOKAWA: *J. Chem. Eng. Jpn*, 1983, **16**, 299–304.
8. A. L. KUNDU, K. M. GUPT, and P. KRISHNA RAO: *Ironmaking Steelmaking*, 1986, **13**, 9–15.
9. A. L. KUNDU, K. M. GUPT, and P. KRISHNA RAO: *Metall. Trans. B*, 1989, **20B**, 581–594.
10. H. TOZAWA, Y. KATO, K. SORIMACHI, and T. NAKANISHI: *ISIJ Int.*, 1999, **39**, 426–434.
11. K. NAKANISHI and J. SZEKELY: *Trans. Iron Steel Inst. Jpn*, 1975, **15**, 522–530.
12. E. FUCHS and P. JÖNSSON: *High Temp. Mater. Process*, 2000, **19**, 333–344.
13. C. VAN DER EIJK, Ø. GRONG, and J. WALMSLEY: Proc. 6th Int. Conf. on 'Molten slags, fluxes and salts', Stockholm, Sweden–Helsinki, Finland, June 2000, KTH, Stockholm, Paper 131.
14. M. GÖRANSSON and P. JÖNSSON: *ISIJ Int.*, 2000, **40**, supplement, 1–5.
15. U. LINDBORG and K. TORSELL: *Trans. AIME*, 1968, **242**, 94–102.
16. R. K. IYENGAR and W. O. PHILBROOK: *Metall. Trans.*, 1972, **3**, 1823–1830.
17. S. LINDER: *Scand. J. Metall.*, 1974, **3**, 137–150.
18. K. HIGASHITANI, R. OGAWA, and G. HOSAKAWA: *J. Chem. Eng. Jpn*, 1982, **15**, 299–304.
19. K. SHIRABE and J. SZEKELY: *Trans. Iron Steel Inst. Jpn*, 1983, **23**, 465–474.
20. D.-Y. SHEN, M. SÖDER, P. JÖNSSON, and L. JONSSON: Proc. 6th Int. Conf. on 'Molten slags, fluxes and salts', Stockholm, Sweden–Helsinki, Finland, June 2000, KTH, Stockholm, Paper 127.
21. 'Slag atlas', 2nd edn; 1995, Düsseldorf, Verlag Stahleisen.
22. A. J. MAJUMDAR: *Trans. J. Br. Ceram. Soc.*, 1964, **63**, 347–364.
23. F. P. GLASSER and J. MARR: *Trans. J. Br. Ceram. Soc.*, 1975, **74**, 113–119.
24. G. HASALL and K. BAIN: Unpublished results, Corus Group, Teesside Technology Centre, Middlesbrough, UK, 1996.
25. N. SHINADA: *Taikabutsu*, 1976, **28**, 371–374.
26. I. D. PRENDERGAST: *Iron Steelmaker*, 1988, **15**, 18–22.
27. J. N. V. T. VAN WIJNAGAARDEN: Proc. 'Electric arc furnace' Conf., 1991, **49**, 361–367.
28. S. RIAZ, K. C. MILLS, and K. BAIN: *Ironmaking Steelmaking*, 2002, **29**, 107–113.
29. O. KNACKE, O. KUBASCHEWSKI, and K. HESSELMANN: 'Thermochemical properties of inorganic substances'; 1991, Heidelberg, Germany, Springer-Verlag.
30. D. R. GASKELL: 'Introduction to metallurgical thermodynamics', 2nd edn. 585–586; 1981, New York, Hemisphere Publishing Corp.
31. E. T. TURKDOGAN: 'Physical chemistry of high temperature technology', 1980, New York, Academic Press.
32. K. BESKOW, N. N. VISWANATHAN, L. JONSSON, and DU SICHEN: *Metall. Trans. B*, 2001, **32B**, 319–328.
33. J. BJÖRKWALL, DU SICHEN, and S. SEETHARAMAN: *Ironmaking Steelmaking*, 2001, **28**, 250–257.
34. G. K. SIGWORTH and J. F. ELLIOTT: *Met. Sci.*, 1974, **8**, 298.
35. C. H. P. LUPIS: 'Chemical thermodynamics of materials'; 1983, New York, North-Holland.
36. D. R. STULL and H. PROPHET: 'JANAF thermochemical tables', 2nd edn; 1971, Washington, DC, US Department of Commerce.
37. I. BARIN: 'Thermochemical data of pure substances'; 1993, Wiesbaden, Wiesbadener Graphische Betriebe.
38. M. W. CHASE, JR, C. A. DAVIES, J. R. DOWNEY, JR, D. J. FRURIP, R. A. MCDONALD, and A. N. SYVERUD: 'JANAF thermochemical tables', 3rd edn, Vol. 14; 1985, Washington, DC, American Chemical Society.
39. R. H. YOON and G. H. LUTRELL: *Miner. Process. Extr. Metall. Rev.,* 1989, **4**, 101–122.
40. H. J. SCHULTZE: *Miner. Process. Extr. Metall. Rev.*, 1989, **5**, 43–76.
41. L. WANG, H.-G. LEE, and P. HAYES: *ISIJ Int.*, 1996, **36**, 7–16.